# Mathematical and Physical Modelling with Dynamic Change in the Center of Gravity of Quadrotor

[1]Mochammad Ariyanto, [1]Munadi
Department of Mechanical Engineering
Diponegoro University, Indonesia
*email: ari_janto5@undip.ac.id

[1,2]Paryanto, [3]Tomohide Naniwa
[2]Institute for Factory Automation and Production Systems
Friedrich-Alexander-Universität Erlangen-Nürnberg, Germany
[3]Department of Human and Artificial Intelligent Systems
University of Fukui, Japan

***Abstract*— One of challenges in aerial grasping is the dynamic change in the center of gravity (CoG). The control system design of quadrotor must be able to compensate for the dynamic change in the CoG of the quadrotor. It is caused when a quadrotor flies and carries a payload, the CoG of quadrotor does not coincide with the center of the quadrotor's geometry. Therefore, for designing a robust control system with respect to an added payload mass, an accurate dynamic model of a quadrotor is highly required. In this paper, the dynamic change in the CoG location of a quadrotor will be developed in mathematical and physical model when the quadrotor carries a payload at hover. The physical model will be utilized to verify the mathematical model. In the simulation of mathematical and physical model, the Euler angle and the altitude of quadrotor are controlled by PID compensator. Based on the simulation results, the quadrotor has the same response especially in transient and steady state responses. For further complex dynamic modelling of quadrotor, physical model can be used for control design purpose with ease of development.**

***Keywords—quadrotor; dynamic model; center of gravity; PID***

## I. INTRODUCTION

The research on quadrotors for aerial grasping has been grown rapidly. At the University of Pennsylvania [1], a quadrotor equipped with gripper to take and carry a light object has been developed. At the University of Utah and the University of California, a quadrotor for aerial manipulation using Proportional–Integral–Derivative (PID) has been developed [2]. Palunko [3] has developed a mathematical model incorporating dynamic change in the center of gravity (CoG) and has synthesized adaptive control to compensate for the dynamic change in CoG. In order to the quadrotor can carry a payload, it is important that the control system can compensate the changes in the location of CoG. Quadrotor dynamic modelling with no payload can be found in literature [4-6]. In references [7] and [8], development of a mathematical model for underwater vehicle incorporating dynamic change in the CoG location can be found. However, most of these researches are still based on the mathematical analysis or experimental investigation. Therefore, these methods are not flexible enough or very difficult when we used to analyze more complex dynamic quadrotor systems. In this research, a complex model with the effect of dynamic change in CoG quadrotor will be developed by using two models, mathematical model and physical model.

In this paper, PID will be used to stabilize the Euler angle and the altitude of quadrotor under an added mass of payload. PID for stabilizing the Euler angle of a quadrotor can be found in literature such as [1-5] and [9] with hardware in the loop (HIL) experiment. In reference [10], a PID compensator is applied to stabilize the Euler angle of both the UAV helicopter and quadrotor. For physical modelling, dynamic modelling using SimMechanics has been published in many sources such as the quadrupedal walking robot [11], helicopter modelling [12], modelling and nonlinear analysis of aircraft ground manoeuvres [13], modelling and simulation of robots based on SimMechanics [14]. In this paper, quadrotor modelling incorporating the dynamic changes of a quadrotor's CoG will be developed with SimMechanics second generation. The physical model will be utilized to verify the mathematical modelling, and furthermore can be used in the advanced dynamics modelling of the quadrotor for more complex dynamics. The quadrotor used as aerial grasping or aerial manipulation is shown in Fig. 1. Based on Fig. 1, the quadrotor can take, carry, and drop a payload which has mass less than 0.4 kg.

(a) (b) (c)

Fig. 1. A quadrotor grasps object: (a) Loading payload (b) Carrying payload (c) Dropping payload

## II. MATHEMATICAL MODELLING

This section will discuss the dynamics modelling of a quadrotor while carrying a payload during hover-flight condition. In the nonlinear model of a quadrotor with a payload, the following was assumed:

- Quadrotor structure is rigid (the system has highly natural frequencies that are not easy to excite) and symmetrical.
- Payload and quadrotor are modelled as a lump mass, which influences the center of mass, or CoG does not coincide with the center of geometry of quadrotor.
- Four propellers are rigid.
- Thrust is linear with the voltage input; four brushless DC motors have high a bandwidth response such that the actuator's dynamic modelling is not needed and modeled as an algebraic equation.
- Drag force opposing the quadrotor body is neglected or small enough because of hovering flight condition.

978-1-5090-4139-8/16/$31.00 ©2016 IEEE

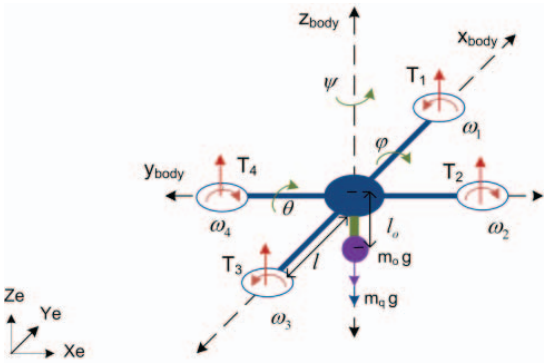


Fig. 2. Quadrotor with payload coordinate system

The movements of a quadrotor having 6 degrees of freedom (DOF), two coordinate frames are defined in Fig. 2 and Fig. 3. The moving coordinate frame {B} is fixed to the quadrotor body and is called the body-fixed reference frame. The origin of the quadrotor frame is chosen to coincide with the CoG when CoG is in the principal plane of quadrotor symmetry. However, when the quadrotor is carrying a payload, it will affect the CoG does not coincide with the principal plane of symmetry, as shown in Fig. 3. The motion of the quadrotor's body-fixed frame is described relative to an inertial reference frame or ground-fixed reference frame {G}.

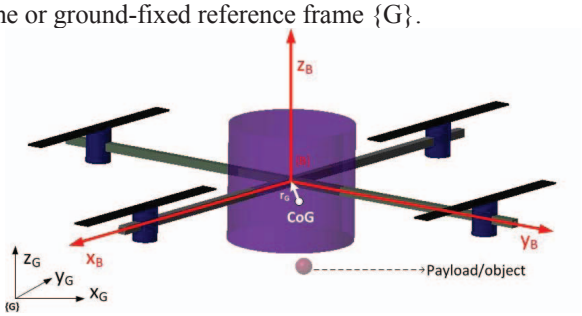


Fig. 3. Quadrotor CoG location change caused by a payload

For quadrotor, it is assumed that the accelerations of a point on the surface of the earth can be neglected. As a result, a ground-fixed reference frame {G} is considered to be inertial. The position and orientation of the quadrotor are described relative to the inertial reference frame {G}. The kinematics of a quadrotor is described with these variables. Equation (1) bellow represents the position of origin *x, y, z* with the quadrotor body-fixed coordinate {B} measured in inertial fixed frame {G}, Equation (2) expresses the Euler angle $\phi,\theta,\psi$ of {B} with respect to {G}, whereas Equation (3) and (4) show translational velocity *u*, *v*, *w* and angular velocity *p*, *q*, *r*, respectively in body-fixed coordinate {B}.

$$\eta_1 = [x \;\; y \;\; z]^T \tag{1}$$

$$\eta_2 = [\varphi \;\; \theta \;\; \psi]^T \tag{2}$$

$$v_1 = [u \;\; v \;\; w]^T \tag{3}$$

$$v_2 = [p \;\; q \;\; r]^T \tag{4}$$

The relation between the earth axes velocity vector ($\dot{\eta}_1$) and body velocity vector $v_1$ can be calculated using Equation (5). In (6), *c* denotes cosine and *s* denotes sine function.

$$\dot{\eta}_1 = \frac{d\eta_1}{dt} = {}^{G}_{B}R(\eta_2)v_1 \tag{5}$$

Where the matrix ${}^{G}_{B}R(\eta_2)$ is a transformation matrix from a body-fixed frame to a inertial-frame obtained by matrix multiplication of the three basic orthogonal rotations. Transformation of linear velocity in {B} to {G} is expressed in (6).

$$\begin{bmatrix}\dot{x}\\ \dot{y}\\ \dot{z}\end{bmatrix} = \begin{bmatrix} c\psi c\theta & -s\psi c\phi + c\psi s\theta s\phi & s\psi s\phi + c\psi s\theta c\phi \\ s\psi c\theta & c\psi c\phi + s\psi s\theta s\theta & -c\psi s\phi + s\psi s\theta c\phi \\ -s\theta & c\theta s\phi & c\theta c\phi \end{bmatrix}\begin{bmatrix}u\\ v\\ w\end{bmatrix} \tag{6}$$

The transformation matrix $Q(\eta_2)$ converts angular body rates $p,q,r$ to Euler angle rate $\dot{\phi},\dot{\theta},\dot{\psi}$. The equation of $Q(\eta_2)$ can be expressed in Equations (7), and (8).

$$\dot{\eta}_2 = \frac{d\eta_2}{dt} = Q(\eta_2)v_2 \tag{7}$$

$$\begin{bmatrix}\dot{\phi}\\ \dot{\theta}\\ \dot{\psi}\end{bmatrix} = \begin{bmatrix} 1 & \sin(\phi)\tan(\theta) & \cos(\phi)\tan(\theta) \\ 0 & \cos(\phi) & -\sin(\phi) \\ 0 & \dfrac{\sin(\phi)}{\cos(\theta)} & \dfrac{\cos(\phi)}{\cos(\theta)} \end{bmatrix}\begin{bmatrix}p\\ q\\ r\end{bmatrix} \tag{8}$$

Finally, the kinematics relationship to transform from a body-fixed coordinate {B} to an inertial-fixed frame coordinate {G} can be calculated using equation (9).

$$\begin{bmatrix}\dot{\eta}_1\\ \dot{\eta}_2\end{bmatrix} = \begin{bmatrix} {}^{G}_{B}R(\eta_2) & 0 \\ 0 & Q(\eta_2) \end{bmatrix}\begin{bmatrix}v_1\\ v_2\end{bmatrix} \tag{9}$$

The new CoG position of $x_G, y_G, z_G$ with respect to the quadrotor body-fixed frame {B} can be written as follows

$$l_o = [l_{ox} \;\; l_{oy} \;\; l_{oz}]^T \tag{10}$$

$$r_G = [x_G \;\; y_G \;\; z_G]^T \tag{11}$$

$$x_G = \frac{m_o l_{ox}}{m+m_o}; y_G = \frac{m_o l_{oy}}{m+m_o}; z_G = \frac{m_o l_{oz}}{m+m_o} \tag{12}$$

$l_o$ is the distance vector between payload and CoG measured from origin of quadrotor CoG. Where *m* and $m_o$ denote mass of quadrotor and payload. $l_{ox}$, $l_{oy}$, and $l_{oz}$ are distance between payload and origin of CoG in $X_B$, $Y_B$, and $Z_B$ axis respectively. The vector $r_G$ represents the CoG position measured from the origin of the body-reference system. The linear acceleration $\dot{u},\dot{v},\dot{w}$ and angular acceleration $\dot{p},\dot{q},\dot{r}$ at the CoG in body-fixed reference coordinate systems is as follows

$$\begin{aligned}
Fx &= m\dot{u} - mvr + mwq - mx_G(q^2+r^2) + my_G(pq-\dot{r}) + mz_G(pr+\dot{q}) \\
Fy &= m\dot{v} - mwp + mur + mx_G(qp+\dot{r}) - my_G(p^2+r^2) + mz_G(qr-\dot{p}) \\
Fz &= m\dot{w} - muq + mvp + mx_G(rp-\dot{q}) + my_G(rq-\dot{p}) - mz_G(q^2+p^2) \\
\tau_x &= I_{xx}\dot{p} + (I_{zz}-I_{yy})qr + m[y_G(\dot{w}-uq+vp) - z_G(\dot{v}-wp+ur)] \\
\tau_y &= I_{yy}\dot{q} + (I_{xx}-I_{zz})rp + m[z_G(\dot{u}-vr+wq) - x_G(\dot{w}-uq+vp] \\
\tau_z &= I_{zz}\dot{r} + (I_{yy}-I_{xx})pq + m[x_G(\dot{v}-wp+ur) - y_G(\dot{u}-vr+wq]
\end{aligned} \tag{13}$$

The matrix representation of a quadrotor's 6 DOF nonlinear dynamic equations of motion can be expressed in compact form as shown in (14).

$$M_B\dot{v} + C_B(v)v = G_B(\eta_2) + U_B \tag{14}$$

The system inertia matrix $M_B$ is as follows

$$M_B\dot{v} = \begin{bmatrix} m & 0 & 0 & 0 & mz_G & -my_G \\ 0 & m & 0 & -mz_G & 0 & mx_G \\ 0 & 0 & m & -my_G & -mx_G & 0 \\ 0 & -mz_G & my_G & I_{xx} & 0 & 0 \\ mz_G & 0 & -mx_G & 0 & I_{yy} & 0 \\ -my_G & mx_G & 0 & 0 & 0 & I_{zz} \end{bmatrix} \begin{bmatrix} \dot{u} \\ \dot{v} \\ \dot{w} \\ \dot{p} \\ \dot{q} \\ \dot{r} \end{bmatrix} \tag{15}$$

Equation (16) exhibits the coriolis-centripetal matrix $C_B(v)$.

$$C_B(v)v = \begin{bmatrix} -mvr + mwq - mx_G(q^2 + r^2) + my_G(pq - \dot{r}) + mz_G(pr + \dot{q}) \\ -mwp + mur + mx_G(qp + \dot{r}) - my_G(p^2 + r^2) + mz_G(qr - \dot{p}) \\ -muq + mvp + mx_G(rp - \dot{q}) + my_G(rq - \dot{p}) - mz_G(q^2 + p^2) \\ (I_{zz} - I_{yy})qr + m[y_G(\dot{w} - uq + vp) - z_G(\dot{v} - wp + ur)] \\ (I_{xx} - I_{zz})rp + m[z_G(\dot{u} - vr + wq) - x_G(\dot{w} - uq + vp] \\ (I_{yy} - I_{xx})pq + m[x_G(\dot{v} - wp + ur) - y_G(\dot{u} - vr + wq] \end{bmatrix} \tag{16}$$

For the input matrix $U_B$ in translational and rotational motion, the thrust generated by the four propellers on body-fixed frame coordinates and the moment caused by four propellers on the $X_B$, $Y_B$, and $Z_B$ body-fixed coordinate of a quadrotor are shown in Equations (17) to (18).

$$U_B = [F_x \; F_y \; F_z \; \tau_x \; \tau_y \; \tau_z \;]^T \tag{17}$$

$$\begin{aligned} F_x &= 0; F_y = 0; F_z = F_1 + F_2 + F_3 + F_4 \\ \tau_x &= l(F_4 - F_2) \\ \tau_y &= l(F_3 - F_1) \\ \tau_z &= M_2 + M_4 - (M_1 + M_3) \end{aligned} \tag{18}$$

Where $F_x$, $F_y$, and $F_z$ are force exerted on $X_B$, $Y_B$, and $Z_B$ body-fixed coordinate of quadrotor. While $\tau_x$, $\tau_y$ and $\tau_y$ are moment exerted on $X_B$, $Y_B$, and $Z_B$ body-fixed coordinate of quadrotor. Force and moment caused by the four motors and propellers are expressed in (19).

$$\begin{aligned} F_i &= a_i v_i + b_i \\ M_i &= c_i v_i + d_i \end{aligned} \tag{19}$$

Where $F$ is the motor's and propeller's thrust and $M$ is moment caused by motors and propellers, where $i$ = 1 to 4 indicates front, right, rear and left motor, $a$ is the thrust coefficient (N/volt), $b$ is the thrust constant (N), $c$ is the moment coefficient (N.m/volt), and $d$ is the moment constant (N.m). Because the CoG does not coincide with the body-fixed frame of the quadrotor, it will cause gravitational moment when the quadrotor flies in a roll and pitch motion. The transformation of the gravitational force $f_G(\eta_2)$ and moment $r_G \times f_G(\eta_2)$ from inertial-fixed frame to a body-fixed frame can be calculated using Equation (20) and (21).

$$f_G(\eta_2) = {}^G_B R^{-1}(\varphi, \theta) \begin{bmatrix} 0 \\ 0 \\ -mg \end{bmatrix} = \begin{bmatrix} mg\sin\theta \\ mg\cos\theta\sin\varphi \\ -mg\cos\theta\cos\varphi \end{bmatrix} \tag{20}$$

$$G_B(\eta_2) = \begin{bmatrix} f_G(\eta_2) \\ r_G \times f_G(\eta_2) \end{bmatrix} = \begin{bmatrix} mg\sin\theta \\ mg\cos\theta\sin\varphi \\ -mg\cos\theta\cos\varphi \\ \begin{bmatrix} x_G \\ y_G \\ z_G \end{bmatrix} \times \begin{bmatrix} mg\sin\theta \\ mg\cos\theta\sin\varphi \\ -mg\cos\theta\cos\varphi \end{bmatrix} \end{bmatrix} \tag{21}$$

The gravitational force and moment vector $G_B(\eta_2)$ in a body-fixed frame coordinate is expressed in Equation (22).

$$G_B(\eta_2) = \begin{bmatrix} mg\sin\theta \\ mg\cos\theta\sin\varphi \\ -mg\cos\theta\cos\varphi \\ -mgy_G\cos\varphi\cos\theta + mgz_G\cos\varphi\cos\theta \\ mgz_G\sin\theta + mgx_G\cos\varphi\cos\theta \\ -mgy_G\sin\theta - mgx_G\cos\theta\sin\varphi \end{bmatrix} \tag{22}$$

(9)

The vector representation of a 6 DOF equation of motion when the quadrotor is carrying a payload can summarized in Equation (23).

$$M_B\dot{v} = M_B{}^{-1}(-C_B(v)v + G_B(\eta_2) + U_B) \tag{23}$$

## III. Physical Modelling

In this study, SimMechanics second generation is used as physical modelling software. SimMechanics allows researchers and engineers to model and simulate a mechanical system with a suite of tools to specify bodies and their mass properties, relative motion, kinematics and dynamics properties of body [15]. In modelling quadrotor dynamics, one of the limitations using SimMechanics is a friction model as drag force that opposes the quadrotor body. The drag force opposing the quadrotor body must be modelled mathematically. When the model is simple, it is more convenient to use the mathematical model than the physical model. In Fig. 4, the top-level quadrotor model is shown which is comprised of a quadrotor body block and configuration, join and sensing. The inputs of the top level model are thrust and moment generated by each motor in the quadrotor body-fixed frame coordinate. The outputs of that block are x, y, z, position in the inertial-fixed frame, Euler angle, and Euler angle rate.

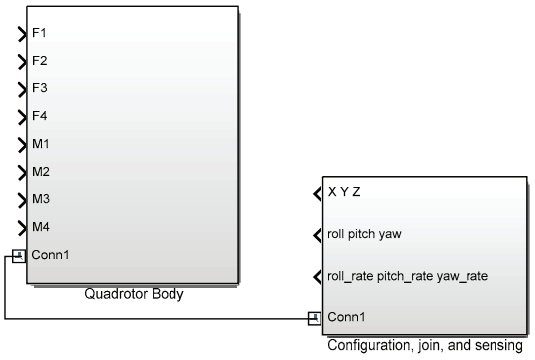


Fig. 4. Top level of quadrotor model in SimMechanics

The configuration, join, and sensing blocks are used for three purposes. The first is utilized as a standard configuration which is comprised of solver configuration, world frame, and mechanism configuration blocks connected to a 6 DOF join. The second purpose is to give the 6 degrees of freedom motion using a 6-DOF Joint block. The third purpose is used for sensing the motion variable, such as the position in the inertial-fixed frame, Euler angle, and Euler angle rate. The physical signal from SimMechanics second generation to Simulink block is converted using PS-Simulink Converter block as shown in Fig. 5.

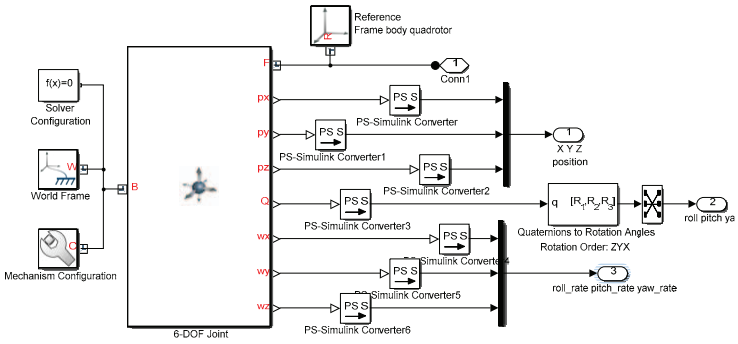


Fig. 5. Block diagram of "configuration, join, and sensing"

Fig. 6 shows the quadrotor body model is comprised of main body, quadrotor frame, motor and propeller, as well as a payload. The payload model and main body uses solid blocks to represent points of mass and solid cylinders, respectively. The properties of the quadrotor body can be seen in Table II, III and IV.

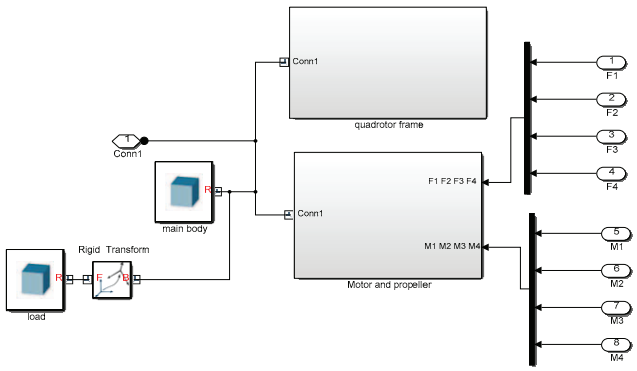


Fig.6. Block diagram of "quadrotor body" with payload

For the quadrotor frame, Fig. 7 consists of two hollow bricks. The hollow bricks can be made using general extrusion techniques in solid block in the SimMechanics environment. A rigid transform block transforms the coordinate of each frame. The transformation is directional and proceeds from the base to the follower frame. Thrust and moment are generated by the motors and propellers in a body fixed-frame coordinate {B}.

From Fig. 8, the thrust and moment input signals from Simulink are converted to physical signals using Simulink P-S Converter. The thrust and moment vector are transformed using a rigid transform block. Thus, the thrust and moment vector are located at the upper middle of the motor and propeller. The motor and propeller are modeled using a solid block with cylinder and brick geometry option, respectively. The differences among the block diagram of "the motor and propeller" front, rear, right, and left are the joint propeller translation and the joint propeller rotation. These joints are used to locate the position of the propeller, as depicted in Table I.

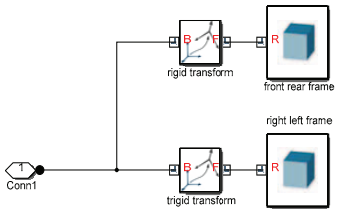


Fig. 7. Block diagram of "quadrotor frame"

TABLE I. JOINT PROPELLER ON QUADROTOR'S FRAME

| Frame | Translation | | | Rotation | |
|---|---|---|---|---|---|
| | X | Y | z | axis | angle |
| Front propeller | 28.5 | 0 | 2 | +X | -90° |
| Rear propeller | -28.5 | 0 | 2 | +X | -90° |
| Left propeller | 0 | -28.5 | 2 | +X | -90° |
| Right propeller | 0 | 28.5 | 2 | +X | -90° |

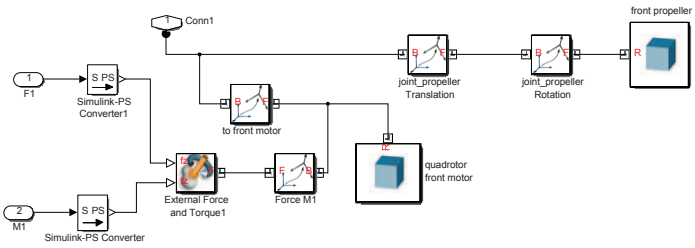


Fig. 8. Diagram block "Front motor and propeller"

After building the model in SimMechanics, it builds a 3D view in SimMechanics explorer automatically, as shown in Fig. 9. It can clearly be seen that the payload changes the position of the CoG which does not coincide with the center of the quadrotor's geometry. Table II summaries the mass properties of the quadrotor component, while Table III and IV summarize the quadrotor symbols and inertia components respectively. The quadrotor center is a quadrotor center which has a cylindrical shape. The quadrotor center is modelled using a solid block in the SimMechanics environment. The quadrotor center has mass and inertia properties which can be filled arbitrarily.

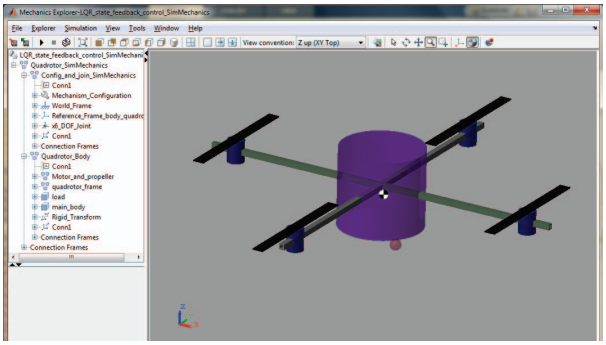

Fig. 9. Quadrotor model with payload in SimMechanics Explorer

TABLE II. MASS OF QUADROTOR COMPONENTS IN SIMMECHANICS

| Compo-nent | Shape | Volume ($cm^3$) | Rho ($gr/cm^3$) | Mass/unit (gr) | Qty | Total mass (gr) |
|---|---|---|---|---|---|---|
| Motor | Cylinder | 28.26 | 4 | 113.04 | 4 | 452.16 |
| Propeller | General extrude | 10 | 0.3 | 3 | 4 | 12.00 |
| Frame | General extrude | 23.76 | 1 | 23.76 | 2 | 47.52 |
| Quadrotor center | Cylinder | 1098.32 | | | 1 | 1098.32 |
| | | Quadrotor total mass | | | | 1,610.00 |

TABLE III. QUADROTOR SYMBOLS IN SIMMECHANICS

| Component | Symbol | Values | Unit |
|---|---|---|---|
| **mass motor** | $m_m$ | **0.11304** | **kg** |
| distance of motor from quadrotor center | $l_m$ | 0.285 | m |
| mass frame | $m_f$ | 0.02376 | kg |
| length of frame | $l_f$ | 0.66 | m |

TABLE IV. QUADROTOR'S INERTIA IN SIMMECHANICS

| | Part | Formula | Inertia ($kg.m^2$) |
|---|---|---|---|
| Roll inertia ($I_{xx}$) | Quadrotor center | | 0.00248 |
| | Motor | $2*m_m*l_m^2$ | 0.018851 |
| | Frame | $2*1/12*m_f*l_f^2$ | 0.000862 |
| | Roll inertia (Ixx) total | | 0.0222 |
| Pitch inertia ($I_{yy}$) | Quadrotor center | | 0.00248 |
| | Motor | $2*m_m*l_m^2$ | 0.018851 |
| | Frame | $2*1/12*m_f*l_f^2$ | 0.000862 |
| | Pitch inertia (Iyy) total | | 0.0222 |
| Yaw inertia ($I_{zz}$) | Quadrotor center | | 0.01157 |
| | motor | $4*m_m*l_m^2$ | 0.037701 |
| | frame | $2*1/12*m_f*l_f^2$ | 0.001725 |
| | Yaw inertia (Iyy) total | | 0.0510 |

## IV. PID COMPENASATOR

A PID compensator design is used to stabilize the quadrotor while carrying a payload under hovering flight conditions, as shown in Fig. 11. PID compensator is used for roll, pitch, yaw, and altitude control. The block diagram of the PID control that is implemented in the mathematical and physical model is shown in Fig. 10.

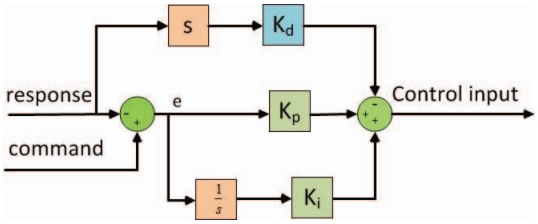


Fig. 10. PID control block diagram of roll control

The PID compensator gains are summarized as shown in Table 5. The gains are implemented in the multi input multi output (MIMO) nonlinear dynamics of the quadrotor as shown in Fig. 11.

TABLE V. TUNED PID COMPENSATOR GAINS

| Control | $k_p$ | $k_d$ | $k_i$ |
|---|---|---|---|
| Altitude | 3 | 0.6 | 0.45 |
| Roll | 0.5 | 0.1 | 0.075 |
| Pitch | 0.5 | 0.1 | 0.075 |
| Yaw | 5 | 1 | 0.75 |

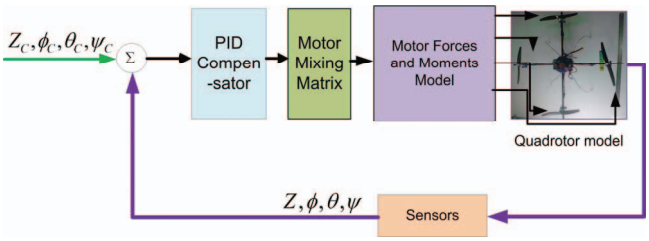


Fig. 11. Block Diagram of quadrotor model with PID Compensator

## V. SIMULATION RESULTS AND CONCLUSSION

A payload is added to both the mathematical and physical model along with an incorporated PID compensator. The mass payload is 0.1 kg and the payload is assumed to be the point of mass. The center of payload is located at 2 cm in *x* positive and 15 cm in *z* negative of the quadrotor body coordinate frame. Fig. 12 and 13 depict the performance of the PID control under an added payload. Fig. 12 shows the Euler angle response given to the doublet input as a reference tracking. Fig. 13 presents the altitude response with step input. It can be seen that the PID control can stabilized the attitude in general and the altitude with reference tracking.

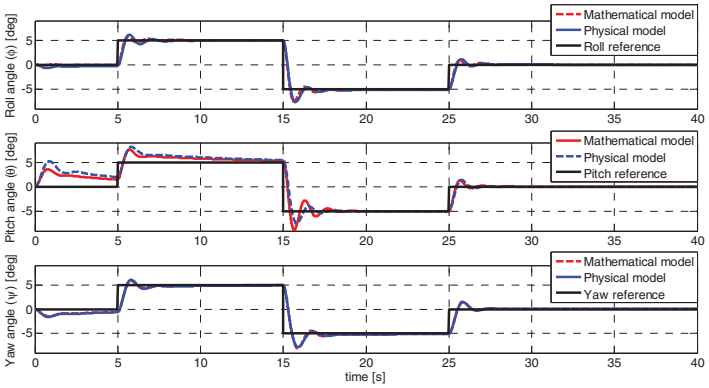


Fig. 12. Euler angle response with 0.1 kg payload

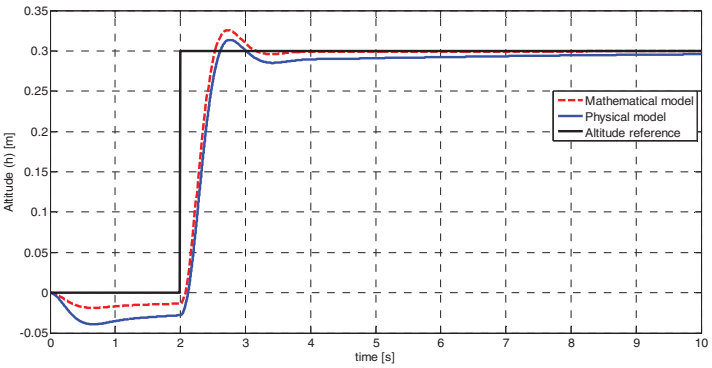


Fig. 13. Altitude response with 0.1 kg payload

The payload is increased in the simulation of both the mathematical and physical model to test the robustness of the PID compensator and to verify the mathematical and physical model. The mass of the payload is 0.2 kg and the payload is assumed to be the point of mass. The center of the payload is located at 2 cm in $x$ positive and 15 cm in $z$ negative of the quadrotor body coordinate frame. Fig. 14 and 15 present the Euler angle response given to the doublet input as a reference tracking and the altitude response with the step input, respectively. It is evident in both the mathematical and physical model that the PID compensator can stabilize the attitude in general and altitude with reference/command tracking. The steady state error is eliminated through the integral action of the PID.

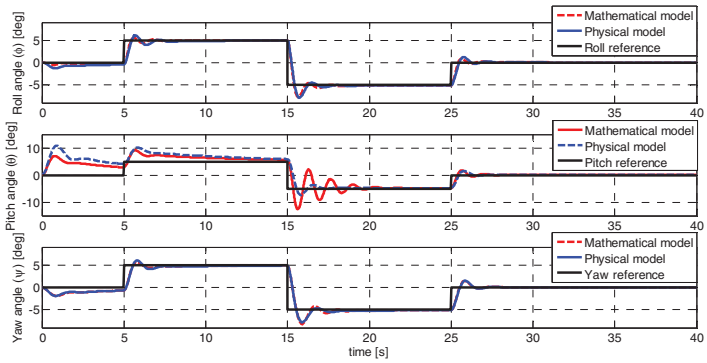


Fig. 14. Euler angle response with 0.2 kg payload

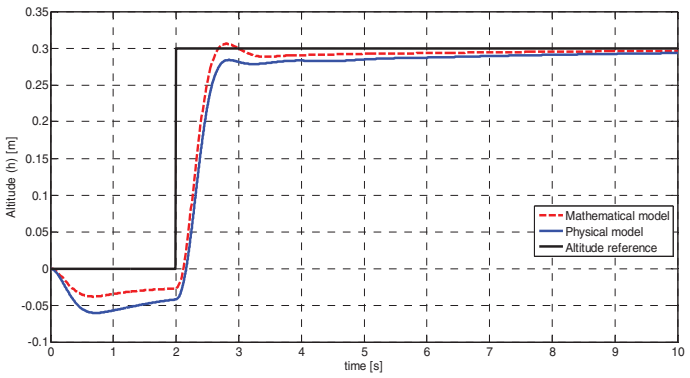


Fig. 15. Altitude response with 0.2 kg payload

Based on the simulation results in both the mathematical and physical model, the quadrotor has the same response especially in transient and steady state responses. The PID compensator can still stabilize the quadrotor with an added payload with a mass up to 0.2 kg located 2 cm in $x$ positive and 15 cm in $z$ negative of the quadrotor body coordinate frame. The PID compensator can also follow the doublet reference/command tracking in roll, pitch, and yaw angle with an added payload. In the Euler angle response and especially in the pitch response, the greater the mass of the payload, the more oscillation occurs in the transient response. With regard to the altitude response, from the simulation results of both the mathematical and physical model it can be summarized that the percentage of overshoot will reduced when the mass of the payload increases. Upon completion of our tests, the mathematical and physical models developed are now ready to use in the advanced and complex dynamic modelling of quadrotor.

## REFERENCES

[1] Q. Lindsey, D. Mellinger and V. Kumar, "Construction with quadrotor teams," Autonomous Robots, vol. 33, no. 3, pp. 323-336, 2012.

[2] V. Ghadiok, J. Goldin and W. Ren , "On the design and development of attitude stabilization, vision-based navigation, and aerial gripping for a low-cost quadrotor," Autonomous Robots, vol. 33, no. 1-2, pp. 41-68, 2012.

[3] I. Palunko and R. Fierro, "Adaptive Control of a quadrotor with dynamic changes in the center of gravity," Proceedings of the 18th IFAC World Congress, pp. 2626-2631, 2011.

[4] S. Bouabdallah, "Design and Control of quadrotors with application to autonomous flying," PhD Thesis, Ecole Polytechnique Federal Lausanne, 2007.

[5] T. Bresciani, "Modelling, identification and control of a quadrotor helicopter," Department of Automatic Control, Lund University, 2008.

[6] J. D. Setiawan, Y. D. Setiawan, M. Ariyanto, A. Mukhtar and A. Budiyono, "Development of real-time flight simulator for quadrotor," Advanced Computer Science and Information Systems (ICACSIS), 2012 International Conference on, Depok, 2012, pp. 59-64.

[7] S. Zhao and J. Yu, "Experimental study on advanced underwater robot control," IEEE Transactions on Robotics, vol. 21, no. 4, pp. 695-703, 2005.

[8] P.J. LeBas, "Maximizing AUV slow speed performance," Master Thesis, MIT, 1997.

[9] A. Güçlü, "Attitude and altitude control of an outdoor quadrotor," Master Thesis, Mechatronics Engineering, Atilim University, 2012.

[10] P.E.I. Pounds, D.R. Bersak and A.M. Dollar, "Stability of small-scale UAV helicopters and quadrotors with added payload mass under PID control," Autonomous Robot, vol. 33, no. 1-2, pp. 129-142, 2012.

[11] Näf, D., "Quadruped walking/running simulation". Semester Thesis. Department of Mechanical and Process Engineering, ETH Zurich, 2011

[12] Ledin, J., Dickens, M., Sharp, J., "Single modeling environment for constructing high-fidelity plant and controller models". In Proceedings of 2003 AIAA Modeling and Simulation Technologies Conference., Austin, 2003

[13] Coetzee, E., "Modeling and Nonlinear Analysis of Aircraft Ground Manoeuvres". PhD Thesis. Department of Engineering Mathematics. University of Bristol, 2011.

[14] Shaoqiang, Y., Zhong, L., Xingshan, L. "Modeling and Simulation of Robot Based on Matlab/SimMechanics" Proceedings of the 27th Chinese Control Conference, 161-165, 2008.

[15] Wood G.D, and Kennedy D.C, "Simulating mechanical systems in Simulink with SimMechanics", Technical report, the Mathworks, Inc, USA, 2003.